Ferracyclic carbamoyl complexes related to the active site of [Fe]-hydrogenase†

Peter J. Turrell, Amanda D. Hill, Saad K. Ibrahim, Joseph. A. Wright and Christopher J. Pickett*

The active site of the [Fe]-hydrogenase features an iron(II) centre bearing *cis* carbonyl groups and a chelating pyridine–acyl ligand. Reproducing these unusual features in synthetic models is an intriguing challenge, which will allow both better understanding of the enzymatic system and more fundamental insight into the coordination modes of iron. By using the carbamoyl group as a surrogate for acyl, we have been able to synthesize a range of ferracyclic complexes. Initial reaction of $Fe(CO)_4Br_2$ with 2-aminopyridine yields a complex bearing a labile solvent molecule, which can be replaced by stronger donors bearing phosphorus atoms to produce a number of derivatives. Introduction of a hydroxy group using this method is unsuccessful both with a free OH group and when this is silyl-protected. In contrast, the analogous reactions starting from 2,6-diaminopyridine does allow synthesis of complexes bearing a pendant basic group.

Introduction

Biologically, activation of dihydrogen occurs by three phylogenetically-distinct types of hydrogenase enzyme: [NiFe], [FeFe]- and [Fe].[1,2] The redox-active [NiFe]- and [FeFe]-hydrogenases have been the focus of studies both at the biological and synthetic levels, with a very large number of models reported for the di-iron system. In contrast, the redox-inactive [Fe]-hydrogenase has to date received less attention. This enzyme catalyses the heterolytic cleavage of dihydrogen into a proton and a hydride, delivering the latter to the substrate methylenetetrahydromethanopterin.[3,4] The crystal structure of the [Fe]-hydrogenase revealed that the iron centre is ligated by an unusual acyl group (Fig. 1).[5,6]

Prior to the confirmation of the structure of the [Fe]-hydrogenase by crystallography, a small number of model compounds had been synthesized based on the available spectroscopic evidence.[7] The design of the majority of these focused on reproduction of a *cis* carbonyl arrangement at iron, and supported the formulation of an iron(II) centre in the enzyme,[8–11] while others introduced pyridine and sulfur ligands around the metal centre.[12,13] Following the publication of the revised crystal structure of the [Fe]-hydrogenase, Hu and coworkers have described the synthesis of five- and six co-ordinate acyl models (Fig. 2)[14–17] and related dimeric sulfur-
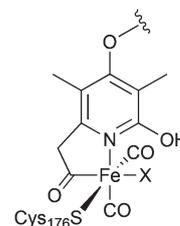
Fig. 1 Active site of the [Fe]-hydrogenase (X = solvent).[6]
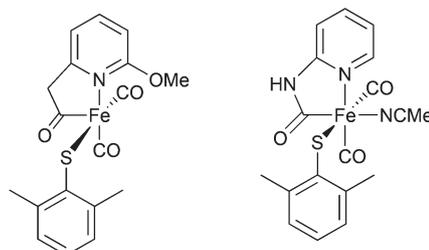
Fig. 2 Monomeric thiolate-containing models of [Fe]-hydrogenase active site reported by Hu and coworkers (left)[15] and Pickett and coworkers (right).[19]

bridged structures.[18] We have communicated a facile route to ferracyclic analogues possessing an intramolecularly-generated carbamoyl group,[19] and described the formation of a thiolate-containing structure which closely reproduces the geometry of the enzyme active site (Fig. 2).

Herein, we now report synthetic and structural details of some new ferracyclic carbamoyl systems, including the

Energy Materials Laboratory, School of Chemistry, University of East Anglia, Norwich Research Park, Norwich, NR4 7TJ, UK. E-mail: c.pickett@uea.ac.uk

identification of a key intermediate in the synthetic pathway, and the first example of a structural model of [Fe]-hydrogenase bearing a basic group at the 6-position on the pyridine ring.

Results and discussion

Formation of carbamoyl ligands has been previously reported following reaction of rhenium and ruthenium carbonyl complexes with amine-substituted nitrogen-containing heterocycles.[20–22] Evidently coordination of the heterocyclic nitrogen atom to the metal centre allows intramolecular attack at an electrophilic CO (Scheme 1). This approach was adapted to synthesise the first ferracyclic carbamoyl structures.

Primary ring-forming reaction

Reaction of $Fe(CO)_4Br_2$ with 2-aminopyridine in CH_2Cl_2 results in the formation of a yellow precipitate **1** with evolution of carbon monoxide (Scheme 2). This material is insoluble in non-coordinating solvents (see below) and was not previously identified.[19] In the coordinating solvent MeCN, **1** reacted to give complex **2** which was fully characterised by X-ray crystallography. Compound **2** provided a starting point for the synthesis of thiolate derivatives related to the active site of [Fe]-hydrogenase (Scheme 2). We have now found that by slow diffusion of a solution of $Fe_2(CO)_4Br_2$ in CH_2Cl_2 into 2-aminopyridine in hexanes we can obtain well-formed crystals of **1** suitable for X-ray analysis. This reveals that **1** is a salt with the anionic component bearing the anticipated carbamoyl functionality and *cis* carbonyl groups: the cationic fragment is a protonated 2-aminopyridine (Fig. 3). The Br–Fe–Br angle in **1** [93.48(3)°] is very similar to that in $Fe(CO)_4Br_2$, [average 92.75(17)°, see ESI† for details], suggesting that the steric requirement of the pyridinyl–carbamoyl ligand is small. The two Fe–Br distances in **1** are significantly different, with the bromide *trans* to the carbamoyl [2.5185(8) Å] longer than that *trans* to a carbonyl [2.4578(9) Å]; the latter is in line with the average
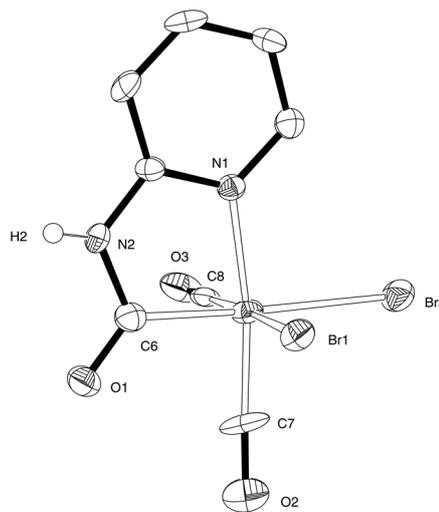

Fig. 3 ORTEP representation of the anion of **1** showing 50% probability ellipsoids; hydrogen atoms except for H(2) have been omitted for clarity. Selected average bond lengths (Å) and angles (°) with estimated standard deviations: Fe(1)–Br(1) 2.4578(9), Fe(1)–Br(2) 2.5185(8), Fe(1)–C(6) 1.921(5), Fe(1)–C(7) 1.769(5), Fe(1)–C(8) 1.844(6), Fe(1)–N(1) 2.004(4); Br(1)–Fe(1)–Br(2) 93.48(3), C(6)–Fe(1)–N(1) 81.78(19), C(7)–Fe(1)–C(8) 89.1(2).

Fe–Br distance in $Fe(CO)_4Br_2$ [2.427(3) Å]. High-resolution mass spectroscopy of *bulk* **1** (formed as the yellow insoluble powder) confirmed the presence of an M^- species at *m/z* 392.7999, with the appropriate isotope pattern for the presence of two bromide groups. The attenuated total reflectance (ATR) infrared spectrum of bulk **1** shows two CO stretches at 1982 cm^{-1} and 2040 cm^{-1} along with a carbamoyl peak at 1660 cm^{-1}.

As reported earlier, dissolution of **1** in MeCN followed by concentration and cooling yielded **2**·MeCN as a crystalline solid (Scheme 2), with X-ray diffraction confirming loss of hydrogen bromide from **1** and retention of the carbamoyl and *cis* carbonyl groups.[19] Here we note that the X-ray structure of **2** shows that the carbamoyl group retains significant double bond character, with the CO bond distance [1.229(3) Å]
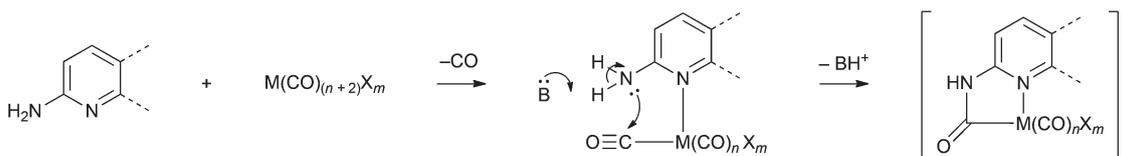
Scheme 1 Generalised mechanism for metallocyclic carbamoyl formation.
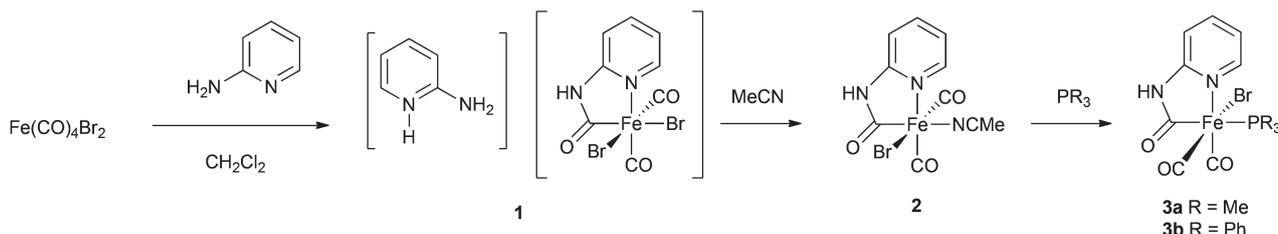

Scheme 2 Synthesis of **3**.

significantly longer than that for the two carbonyls [1.136(3) Å and 1.086(3) Å] but shorter than would be anticipated for a C–O single bond. The C–N distance [1.383(3) Å] also confirms the partial double-bond character of this unit. Examination of the C–Fe and N–Fe bond lengths in **1** and **2** shows that they are not significantly different, whilst the C–Fe–N angles in the two compounds are very similar [81.84(18)° and 82.68(9)°, respectively]. The carbamoyl ligand unit is therefore insensitive to the wider metal environment: with the exception of compound **3a** (*vide infra*), this pattern is seen for all of the monomeric carbamoyl complexes we have examined.

Substitution chemistry of complex 2

Complex **2** possesses a potential labile solvato ligand, MeCN. We have shown that this can be replaced by THF and reversibly by CO:[19] here we further explore the substitution of the solvato ligands MeCN and THF with phosphines.

Slow addition of a dilute solution of PMe_3 to **2** in THF enabled the isolation of **3a** in which the ligating solvent is replaced by the phosphine ligand (Scheme 2, Fig. 4). Compared to complexes **1** and **2**, the carbamoyl ligand in **3a** is 'twisted' such that the pyridine ring does not lie directly above the Fe–P bond, reducing steric clash between the phosphine and pyridine groups. In solution, the IR spectrum of **3a** shows maxima at 1934 cm^{-1}, 1967 cm^{-1} and 2035 cm^{-1}, absorptions which are shifted to lower wavenumbers with respect to the parent complex and indicative of better electron-donating ability of the PMe_3 ligand compared with MeCN at the Fe(II) centre.

Reaction of **2** with PMe_3 in THF is evidently sensitive to moisture and/or oxygen, as a by-product which co-crystallised with **3a**, $[Fe(MeCN)_4(PMe_3)_2][(Br_3Fe)_2O]$, has been identified, in
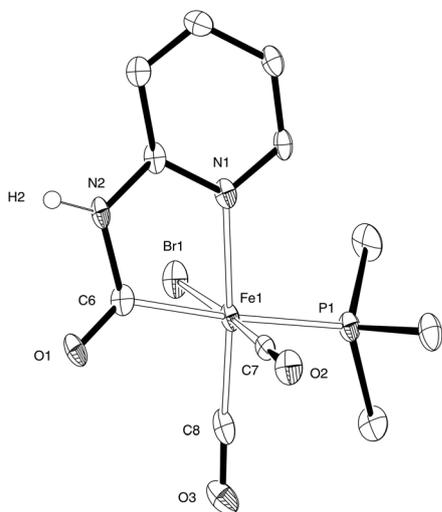
which the carbamoyl ligand has been lost entirely from the metal centre (see ESI†).

The reaction of **2** in THF with one equivalent of PPh_3 gave a mixture of mono- and di-substituted compounds. Modifying the reaction procedure by carrying out and working up under an atmosphere of CO allowed isolation of **3b**, which exhibits solution IR stretches at 2040 cm^{-1} and 1990 cm^{-1} in the carbonyl region. Compound **3b** gave satisfactory elemental analysis to support formulation as the monophosphine. The di-substituted complex $Fe(CO)(PPh_3)_2(Br)(C_6H_5N_2CO)\cdot THF$ was isolated as a minor product which was characterized by crystallography (see ESI†).

Basic functionality at the 6-position of the pyridine ring

With a secure route to models replicating the first coordination sphere of the active site of the [Fe]-hydrogenase, the next target is replicating the wider environment around the iron. The native enzyme contains a hydroxyl group pendant to the putative hydrogen bind site,[6] and the involvement of this group in catalysis has been proposed.[4] Theoretical studies suggest that the lone pair of the oxygen sufficiently basic enough to able to polarize the hydrogen–hydrogen bond, facilitating hydrogen activation.[23,24]

Based on the formation of **1** by reaction of 2-aminopyridine with $Fe(CO)_4Br_2$, we sought to introduce a hydroxy group using **4a** as the ligand precursor. Compound **4a** (Fig. 5) has previously been synthesized from 2,6-diaminopyridine by reaction with HCl[25] or H_2SO_4,[26] but in neither case is spectroscopic data available. Modification of the procedure of Tisza and Joos[25] allowed us to reliably access **4a** in good yield. We have established by an X-ray diffraction study that **4a** exists as the keto form **4a'** in the solid state (see ESI†), but this does not interfere with the reactivity of the hydroxy group in solution (see below). Reaction of **4a** with $Fe(CO)_4Br_2$ led to a very rapid reaction with significant effervescence; IR indicated that all bound CO had been lost in this process. Attempts to moderate the reaction by cooling and dilution were unsuccessful. To exclude the possibility that this failure was due to reaction at two competing sites, we moved to protection of the hydroxyl group in **4a**. Silylation using $(i-Pr)_3SiCl$ under standard conditions to yield **4b** proceeded smoothly. However, reaction of **4b** with $Fe(CO)_4Br_2$ gave similar results to that with **4a**: loss of carbonyl signals in the infrared. It is possible that HBr liberated in the formation of the carbamoyl is able to attack the silyl group, deprotecting *in situ* and thus leading to the same reactivity seen with **4a**.

Fig. 4 ORETP representation of the structure of **3a** showing 50% probability ellipsoids; hydrogen atoms except for H(2) have been omitted for clarity. Selected average bond lengths (Å) and angles (°) with estimated standard deviations: Fe(1)–Br(1) 2.4914(6), Fe(1)–C(6) 1.981(3), Fe(1)–C(7) 1.760(4), Fe(1)–C(8) 1.779(4), Fe(1)–N(1) 2.006(3), Fe(1)–P(1) 2.3152(10); C(7)–Fe(1)–C(8) 90.19(16), C(6)–Fe(1)–N(1) 82.10(13), Br(1)–Fe(1)–P(1) 87.86(3).
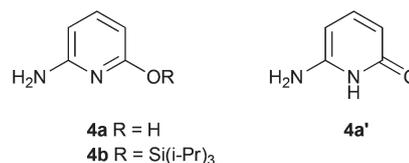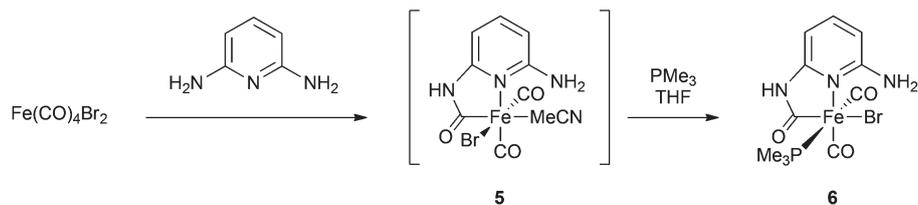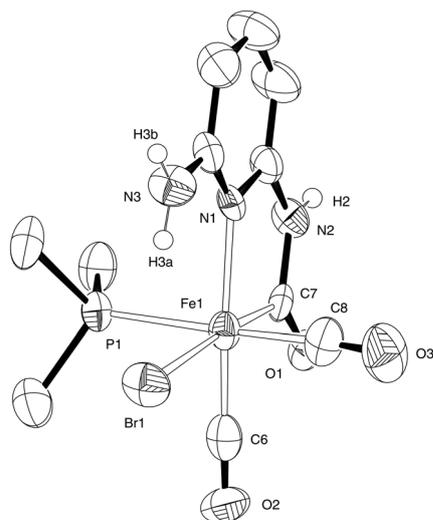

Fig. 5 Oxygen-functionalised aminopyridines.

Scheme 3 Synthesis of **6**.

Fig. 6 ORTEP representation of the structure of **6**·MeCN showing 50% probability ellipsoids; hydrogen atoms except for H(2), H(3a) and H(3b) have been omitted for clarity. Selected average bond lengths (Å) and angles (°) with estimated standard deviations: Fe(1)–Br(1) 2.5488(18), Fe(1)–C(6) 1.917(11), Fe(1)–C(7) 1.789(13), Fe(1)–C(8) 1.826(14), Fe(1)–N(1) 2.077(8), Fe(1)–P(1) 2.270(3); C(6)–Fe(1)–N(1) 82.5(4), C(7)–Fe(1)–C(8) 92.8(5).

We therefore turned to the introduction of an alternative basic group in the form of the second amine group in 2,6-aminopyridine. Carbamoyl formation on one side of this molecule would be expected to leave the second amine group free to participate in further chemistry. Following a similar procedure to that which produces compound **2**, the diamine was added to a solution of $Fe(CO)_4Br_2$ (Scheme 3). Effervescence due to the liberation of carbon monoxide was observed and a pale yellow precipitate was rapidly formed. Dissolution of the yellow powder in MeCN gave a solution showing CO stretching frequencies at 1999 cm^{-1} and 2055 cm^{-1}; this was tentatively assigned as **5**. Even when stored in the dark at −20 °C, solutions of **5** were unstable whilst evaporation of the solvent left only intractable oils, precluding the acquisition of further data. We therefore added PMe_3 directly to a crude preparation of **5** in THF, leading to the appearance of new IR bands at 1963 cm^{-1}, 1985 cm^{-1} and 2042 cm^{-1}. When crystallized from concentrated solutions,‡ compound **6** (Fig. 6) was obtained as

orange blocks. A diffraction study confirmed the presence of a free amino group in this material, along with retention of the *cis* carbonyl arrangement as required. The geometry at iron is similar to the other carbamoyl complexes reported here, although it is notable that the bromide occupies the position *trans* to the carbamoyl here, in contrast to the arrangement in **3**. This arrangement permits intramolecular hydrogen bonding to take place, with an H(3a)···Br(1) distance of 2.36 Å. The other protic hydrogen atoms in **6** are involved in intermolecular interactions as would be expected.

Electrochemistry

Cyclic voltammetry of **2** in MeCN-0.1 M [NBu$_4$][BF$_4$] at vitreous carbon revealed irreversible waves for both oxidation and reduction. Oxidation gave a single wave at $E_{p,ox}$ = +1.36 V *versus* Ag/AgCl, while reduction showed two waves at −1.17 V and −1.43 V *versus* Ag/AgCl. Notably the natural centre in the enzyme is redox inactive in the accessible physiological potential domain *ca* −1.0 to +1.0 V *versus* Ag/AgCl, and the observed oxidation and reduction potentials of the synthetic complex is in accord with this. The large HOMO–LUMO gap of some 2.5 V is indicative of the stability of the Fe(II) structure *cf.* Pearson's principle of maximum hardness.[27] Cyclic voltammetry of **3a** similarly revealed only irreversible oxidation and reduction processes at E_p^{ox} = +1.26 V and E_p^{red} = −1.36 V *versus* Ag/AgCl, respectively. Infrared spectroelectrochemistry of **3a** in the MeCN electrolyte showed depletion bands at $E_{applied}$ = E_p but the absence of detectable growth bands in the CO region, indicative of oxidative decarbonylation on the seconds timescale.

Conclusions

Metallocyclic carbamoyl complexes are rare. We have now identified and structurally characterised a key precursor on a pathway which has provided access to a range substituted ferracyclic structures, including new phosphine derivatives (Scheme 2). In the [Fe]-hydrogenase structure nature deploys a hydroxyl-ketonic group at the 6-position on the pyridine ring in a ferracyclic structure and this is thought to be important in heterolytic cleavage of dihydrogen acting as proton acceptor. Although approaches to synthesise a synthetic analogue with a similar framework were unsuccessful, we have shown that the reaction of $Fe(CO)_4Br_2$ with 2,6-diaminopyridine affords a ferracyclic structure which has a basic amino group juxtaposed in the 6-position to the Fe centre, *i.e.* in the second

‡When crude **6** is crystallized slowly from dilute solution, partial decomposition takes place leading to the isolation of Fe(CO)(PMe$_3$)$_2${C$_6$H$_6$N$_3$CO(FeBr$_3$)}(MeCN). This dinuclear material features a FeBr$_3^-$ group bound to the carbamoyl oxygen. See ESI† for further details.

coordination sphere, and this complex has been structurally characterised.

Experimental

General

Unless otherwise stated, reactions were carried out under nitrogen using conventional air-sensitive techniques. Starting materials were purchased from Aldrich or Alfa Aesar and were used without further purification. Solvents were freshly distilled under an inert atmosphere of N_2 from an appropriate drying agent. NMR spectra were recorded at 25 °C in 5 mm tubes using a Bruker Avance 300 spectrometer. FT-IR spectra were recorded on a Perkin-Elmer SpectrumBX instrument, fitted with a SensIR Technologies DuraSamplIR II ATR unit where appropriate. Elemental analyses were performed by London Metropolitan University. Cyclic voltammetric measurements were carried out using an Autolab PGSTAT 30 potentiostat. A conventional three-electrode arrangement was employed, consisting of a vitreous carbon working electrode, a platinum wire as the auxiliary electrode, and Ag/AgCl as a reference electrode. All measurements were done in dry degassed MeCN in the presence of 0.1 M $[NBu_4][BF_4]$ as the supporting electrolyte at room temperature. Spectroelectrochemistry experiments were carried out using a Spectroelectrochemistry Partners SP-02 cell mounted on a Pike MIRacle ATR unit fitted to a Bruker Vertex 80 spectrometer.

$Fe(CO)_4Br_2$

This was synthesized as previously reported.[19] Crystals suitable for X-ray diffraction were grown by sublimation at reduced pressure.

$[C_5H_7N_2][Fe(C_6H_5N_2O)(CO)_2Br_2)]$ (1)

A solution of 2-aminopyridine (12 mg, 0.13 mmol) in hexane (5 cm^3) was carefully layered onto a solution of $Fe(CO)_4Br_2$ (50 mg, 0.13 mmol) in CH_2Cl_2 (10 cm^3). A small amount (ca 5 mg) of yellow crystalline $[C_5H_7N_2][Fe(C_6H_5N_2O)(CO)_2Br_2)]$ was formed upon the slow diffusion of the solutions through each other over the course of five days and the isolated material was characterized by X-ray diffraction. Found C 30.11, H 2.31, N 11.01%; $C_{13}H_{12}Br_2FeN_4O_3 \cdot 0.5(CH_2Cl_2)$ requires C 30.57, H 2.47, N 10.56%. m/z (orbitrap) calcd for anion $C_8H_5N_2Br_2FeO_3$ 392.8001, found 392.7999.

$FeBr(C_6H_5N_2O)(CO)_2(PMe_3)$ (3a)

A solution of PMe_3 (0.065 cm^3, 0.063 mmol) dissolved in THF (10 cm^3) was added drop wise to 2 (240 mg 0.607 mmol) in THF (10 cm^3) over 30 minutes. During the addition, the solution turned from orange-red to a darker red-purple. The volume of the solution was reduced to 2 cm^3 under vacuum before cooling to −20 °C. A white solid precipitated; the supernatant was decanted and the solvent was removed under reduced pressure yielding a sticky oil. This was taken in MeCN (ca 1 cm^3) and evaporated in vacuum three times to co-

evaporate the residual THF. The solid was recrystallized from a minimum of MeCN at −20 °C, give of red crystals of X-ray quality (8 mg, 3%). Found C 34.04, H 3.55, N 7.12%; $C_{11}H_{14}BrFeN_2O_3P$ requires C 33.95, H 3.63, N 7.20%. $\nu_{max}/$cm^{-1} (MeCN) 2035, 1967, 1934. m/z (CI$^-$) 361.8, 359.9 (M − H − CO). ^{31}P NMR (121 MHz, CD_2Cl_2): δ −12.51.

$FeBr(C_6H_5N_2O)(CO)_2(PPh_3)$ (3b)

Solid PPh_3 (211 mg, 0.805 mmol) was added to 2 (316 mg 0.805 mmol) in THF (20 cm^3). The solvent volume was reduced by sparging with CO, leading to the formation of a red-brown precipitate. The final brown paste was washed with cold THF (−20 °C, 5 cm^3) to leave a red-brown powder (315 mg, 68%). Found C 54.19, H 3.60, N 4.89%; $C_{26}H_{20}BrFeN_2O_3P$ requires C 54.29, H 3.50, N 4.87%. $\nu_{max}/$cm^{-1} (THF) 2040, 1990, 1666, 1620. ^{31}P NMR (121 MHz, CD_2Cl_2): δ 37.47.

6-Aminopyridin-2-ol (4a)

2,6-Diaminopyridine (12.5 g, 114 mmol) was refluxed in HCl (10%, 300 cm^3) for three hours. The solvent was distilled out at atmospheric pressure to leave 50 cm^3 of concentrated solution. On cooling, a pale crystalline material precipitated and was recovered by filtration. The crude material was redissolved in a minimum of hot water and the pH adjusted to 11 by addition of 40% NaOH solution. Cooling to 0 °C led to the formation of needle-like crystals of the product. After washing with CH_2Cl_2, this was recrystallized from hot water (4.0 g, 32%). Crystals suitable for X-ray diffraction were obtained from this second crystallization. ^1H NMR (300 MHz, D_2O): δ 5.54 (m, 1H), 5.57 (d, 1H, J = 3.9 Hz), 7.23 (t, 1H, J = 8.3 Hz). ^{13}C NMR (75 MHz, D_2O): 92.23, 101.81, 145.75, 151.59, 163.81. m/z (EI+) 110.0.

6-{[Tris(propan-2-yl)silyl]oxy}pyridin-2-amine (4b)

6-Aminopyridin-2-ol 4a (618 mg, 5.62 mmol) was dissolved in THF (100 cm^3) and cooled to −78 °C. Butyl lithium (1.6 M in THF, 3.51 cm^3) was added slowly, and the reaction stirred for 2 h before warming to room temperature. Tris(isopropyl)silyl chloride (1.20 cm^3, 5.62 mmol) was added, and reaction stirred for 48 h. The solvent was removed at reduced pressure and the product extracted from the residue with CH_2Cl_2. This was then filtered and the solvent removed at reduced pressure to leave a yellow/brown oil, which was used directly (910 mg, 61%). ^1H NMR (300 MHz, CD_2Cl_2): δ 1.10 (d, 27H, J = 7.4 Hz), 1.35 (octet, 3H, J = 7.4 Hz), 6.04 (d, 1H, J = 1.7 Hz), 6.07 (d, 1H, J = 1.7 Hz), 7.32 (t, 1H, J = 7.8 Hz). m/z (orbitrap) calcd for $C_{14}H_{25}N_2OSi$ 267.1887, found 267.1892.

$FeBr(C_6H_6N_3O)(CO)_2(PMe_3)$ (6)

Solid 2,6-diaminopyridine (186 mg, 1.71 mmol) was added to a solution of $Fe(CO)_4Br_2$ (560 mg, 1.71 mmol) in CH_2Cl_2 (25 cm^3); gas was evolved and a precipitate formed. After two hours, the precipitate was recovered by filtration and dried in vacuo; this gave 557 mg of yellow solid. The solid was taken up in THF (10 cm^3), and a solution of PMe_3 (0.14 cm^3, 1.35 mmol) in THF (15 cm^3) was added. After one hour, the volume was reduced to approximately 5 cm^3 and the solution

Table 1 Summary of crystallographic data for Fe(CO)$_4$Br$_2$, **1**, **3a** and **6**·MeCN

	Fe(CO)$_4$Br$_2$	1	3a	6·MeCN
Formula	C$_4$Br$_2$FeO$_4$	C$_8$H$_5$Br$_2$FeN$_2$O$_3$, C$_5$H$_7$N$_2$	C$_{11}$H$_{14}$BrFeN$_2$O$_3$P	C$_{11}$H$_{15}$BrFeN$_3$O$_3$P, C$_2$H$_3$N
M	327.71	487.94	388.97	445.04
Space group	$C2$	$P2_1/n$	$P2_1/a$	$P2_1/c$
a/Å	6.7608(4)	11.2197(6)	13.2378(3)	9.8203(17)
b/Å	10.2296(5)	12.6286(7)	7.5324(3)	12.719(2)
c/Å	12.2954(7)	11.8538(6)	15.4174(5)	15.139(2)
β/°	103.801(3)	105.142(5)	110.218(2)	91.830(14)
V/Å^3	825.80(8)	1621.24(15)	1442.58(8)	1890.0(5)
T/K	120(2)	140(2)	120(2)	140(2)
Z	4	4	4	4
R_{int}	0	0.074	0.056	0.165
R_1 [$I > 2\sigma_I$]	0.068	0.042	0.040	0.091
wR_2 (all data)	0.177	0.085	0.079	0.277

cooled to −20 °C overnight. The solution was filtered to remove any white precipitate that had formed, then dried under vacuum to give a sticky orange oil. Recrystallization of this oil from a minimum of MeCN (∼3 cm^3) at −20 °C gave a mass of homogeneous crystals of **8** (51 mg, 7.5%). Compound **6** was isolated as orange blocks suitable for X-ray diffraction study. Found C 32.46, H 3.89, N 10.21%; C$_{11}$H$_{16}$BrFeN$_3$O$_3$P requires C 32.62, H 3.98, N 10.38%. ν_{max}/cm^{-1} (THF) 1963, 1985, 2042. m/z (CI$^-$) 376.9, 374.9 (M − H − CO).

Crystallography

Crystals were suspended in oil, and one was mounted on a glass fibre and fixed in the cold nitrogen stream of the diffractometer. Data were collected an Oxford Diffraction Xcalibur-3 CCD diffractometer equipped with Mo-Kα (λ = 0.71073 Å) radiation and graphite monochromator (**1** and **6**·MeCN), or a Bruker–Nonius FR591 molybdenum rotating anode and confocal mirrors [Fe(CO)$_4$Br$_2$ and **3a**]. Data were processed using the CrysAlisPro program (**1** and **6**·MeCN)[28] or the DENZO and COLLECT programs [Fe(CO)$_4$Br$_2$ and **3a**].[29] Structures were determined by the direct methods routines in the Superflip program[30] (**1** and **3a**) or SHELXS program[31] [Fe(CO)$_4$Br$_2$ and **6**·MeCN], and were refined by full-matrix least-squares methods on F^2 in SHELXL.[31] Non-hydrogen atoms were refined with anisotropic thermal parameters. Hydrogen atoms bound to nitrogen were located in the Fourier difference map and freely refined where possible; in all other cases they were included in idealized positions and their U_{iso} values were set to ride on the U_{eq} values of the parent carbon atoms. Crystallographic data for previous-unpublished structures are summarized in Table 1 and S1† (ESI†). CCDC 922917–922924 contain the supplementary crystallographic data for Fe(CO)$_4$Br$_2$, **1**, **3a** and **6**·MeCN and the supporting structures.

References

1 C. Tard and C. J. Pickett, *Chem. Rev.*, 2009, **109**, 2245–2274.
2 J.-F. Capon, F. Gloaguen, F. Y. Pétillon, P. Schollhammer and J. Talarmin, *Coord. Chem. Rev.*, 2009, **253**, 1476–1494.
3 S. Shima and U. Ermler, *Eur. J. Inorg. Chem.*, 2011, 963–972.
4 M. J. Corr and J. A. Murphy, *Chem. Soc. Rev.*, 2011, **40**, 2279–2292.
5 S. Shima, O. Pilak, S. Vogt, M. Schick, M. S. Stagni, W. Meyer-Klaucke, E. Warkentin, R. K. Thauer and U. Ermler, *Science*, 2008, **321**, 572–575.
6 T. Hiromoto, K. Ataka, O. Pilak, M. S. Stagni, W. Meyer-Klaucke, E. Warkentin, R. K. Thauer, S. Shima and U. Ermler, *FEBS Lett.*, 2009, **583**, 585–590.
7 J. A. Wright, P. J. Turrell and C. J. Pickett, *Organometallics*, 2010, **29**, 6146–6156.
8 Y. Guo, H. Wang, Y. Xiao, S. Vogt, R. K. Thauer, S. Shima, P. I. Volkers, T. B. Rauchfuss, V. Pelmenschikov, D. A. Case, E. E. Alp, W. Sturhahn, Y. Yoda and S. P. Cramer, *Inorg. Chem.*, 2008, **47**, 3969–3977.
9 B. V. Obrist, D. Chen, A. Ahrens, V. Schünemann, R. Scopelliti and X. Hu, *Inorg. Chem.*, 2009, **48**, 3514–3516.
10 X. Wang, Z. Li, X. Zeng, Q. Luo, D. J. Evans, C. J. Pickett and X. Liu, *Chem. Commun.*, 2008, 3555–3557.
11 T. Liu, B. Li, C. V. Popescu, A. Bilko, L. M. Pérez, M. B. Hall and M. Y. Darensbourg, *Chem.–Eur. J.*, 2010, **16**, 3083–3089.
12 A. M. Royer, M. Salome-Stagni, T. B. Rauchfuss and W. Meyer-Klaucke, *J. Am. Chem. Soc.*, 2010, **132**, 16997–17003.
13 D. Chen, R. Scopelliti and X. Hu, *J. Am. Chem. Soc.*, 2010, **132**, 928–929.
14 D. Chen, R. Scopelliti and X. Hu, *Angew. Chem., Int. Ed.*, 2010, **49**, 7512–7515.
15 D. Chen, R. Scopellitti and X. Hu, *Angew. Chem., Int. Ed.*, 2011, **50**, 5671–5673.

16 D. Chen, A. Ahrens-Botzong, V. Schünemann, R. Scopelliti and X. Hu, *Inorg. Chem.*, 2011, **50**, 5249–5257.

17 D. Chen, R. Scopelliti and X. Hu, *Angew. Chem., Int. Ed.*, 2012, **51**, 1919–1921.

18 B. Hu, D. Chen and X. Hu, *Chem.–Eur. J.*, 2012, **18**, 11528–11530.

19 P. J. Turrell, J. A. Wright, J. N. T. Peck, V. S. Oganesyan and C. J. Pickett, *Angew. Chem., Int. Ed.*, 2010, **49**, 7508–7511.

20 J.-L. Zuo, W.-F. Fu, C.-M. Che and K.-K. Cheung, *Eur. J. Inorg. Chem.*, 2003, 255–262.

21 P. Nombel, N. Lugan, B. Donnadie and G. Lavigne, *Organometallics*, 1998, **18**, 187–196.

22 Formation of a carbamoyl heterocycle on ruthenium has also been described by electrochemical reduction: T. Tomon, T.-A. Koizumi and K. Tanaka, *Angew. Chem., Int. Ed.*, 2005, **44**, 2229–2232.

23 X. Yang and M. B. Hall, *J. Am. Chem. Soc.*, 2009, **131**, 10901–10908.

24 A. Dey, *J. Am. Chem. Soc.*, 2010, **132**, 13892–13901.

25 E. T. Tisza and B. Joos, *US Patent*, 1863676, 1932.

26 O. A. Seide and A. I. Titow, *Ber. Dtsch. Chem. Ges.*, 1936, **69**, 1884–1893.

27 R. G. Pearson, *Acc. Chem. Res.*, 1993, **26**, 250–255.

28 *CrysAlisPro*, Oxford Diffraction Ltd., Abingdon, UK, 2010.

29 Z. Otwinowski and W. Minor, in *Methods in Enzymology*, ed. C. W. Carter Jr. and R. M. Sweet, Academic Press, New York, 1997, vol. 276, pp. 307–326.

30 L. Palatinus and G. Chapuis, *J. Appl. Crystallogr.*, 2007, **40**, 786–790.

31 G. M. Sheldrick, *Acta Crystallogr., Sect. A: Fundam. Crystallogr.*, 2008, **64**, 112–122.

32 S. J. Coles and P. A. Gale, *Chem. Sci.*, 2012, **3**, 683–689.